Oil Shale, 2026, 43, 2, 143–164 https://doi.org/10.3176/oil.2026.2.02

Heat transfer optimization in oil shale rotary retorting via DEM and BP neural network

Sitong Liu[(a)], Naying Yuan[(a)], Chunhua Wang[(a)]*, Yubaodan Sun[(b)], Ninging Li[(a)]*, Yue Yue[(a)], Haodan Pan[(a)], Zhiyong Hu[(a)], Lei Zhao[(a)]

[(a)] College of Mechanical Engineering, Liaoning Petrochemical University, Fushun, 113001, China

[(b)] Hubei Institute of Aerospace Chemotechnology, Xiangyang, 441003, China

Received 3 August 2025, accepted 8 April 2026, available online 16 April 2026

Abstract. *To enhance heat transfer between shale ash and oil shale particles in a rotary retorting furnace, this study coupled the discrete element method (DEM) with a particle heat conduction model to simulate mixing and heat transfer, examining the effects of particle filling ratio, furnace rotational speed, and baffle structures. A backpropagation neural network (BP-NN) model was built from simulation data to map furnace operation time with key parameters, and a genetic algorithm was used to optimize parameters to minimize operation time. The research results show that lower filling degrees and higher rotation speeds significantly strengthen particle mixing and heat exchange, which accelerate the system's stabilization, improve temperature field uniformity, and reduce the temperature standard deviation. The mixing and heat transfer effect of the straight baffle is between that of the right-angle baffle and the inclined baffle, but it causes the largest temperature standard deviation. In contrast, the right-angle baffle demonstrates stronger advantages in heat transfer uniformity during particle lifting and throwing. The constructed BP-NN prediction model achieves a relative error accuracy within 0.25%, effectively solving the long computation time problem of DEM simulation. The optimized parameter combination provides a theoretical basis for the development of high-efficiency and energy-saving rotary retorting furnaces.*

Keywords**:** *oil shale, rotary retorting furnace, DEM, BP-NN.*

1. Introduction

Oil shale is a type of sedimentary rock containing a substance known as kerogen, which can be converted to liquid hydrocarbons through thermal treatment [1, 2]. Despite its low energy density and high production cost, oil shale, as

* Corresponding authors, wangchunhua@lnpu.edu.cn, lining773239@163.com

a non-conventional oil source, is rich in reserves and widely distributed [3, 4]. This is of strategic importance, as it can effectively supplement traditional fossil energy, reduce dependence on imported oil, enhance energy security, and promote the diversification of the energy structure. At present, Estonia, Brazil, the United States, and other countries have advanced oil shale processing technologies and have realized its industrial utilization. China has also carried out oil shale processing in Fushun, Xinjiang, and Gansu, among which Fushun has the largest annual production of shale oil [5].

The operational performance of an oil shale rotary retorting furnace (abbreviated as a rotary furnace here), as an efficient thermal conversion equipment, directly depends on the synergistic optimization of particle mixing and heat transfer efficiency [6–8]. Studies have shown that conventional operating parameters such as rotational speed, particle filling degree, and baffle shape have a significant effect on the particle flow pattern and heat transfer characteristics in the furnace [9–11]. Zhang et al. [12] experimentally investigated the mixing behavior of unequal particle size oil shale and solid heat carrier particles in a rotary furnace. They found that, when convective mixing was predominant, the mixing degree was better under the condition of using a right-angle baffle with a 20% filling degree and an inclination angle of 3.24° than under other corresponding conditions. Herz et al. [13] experimentally investigated the influence of rotational speed and filling degree on the contact heat transfer coefficient in rotary furnaces, revealing that the heat transfer coefficient increased with higher rotational speeds and lower filling degrees.

The optimization of reactor structure is equally crucial for enhancing processing efficiency and enabling the treatment of diverse feedstocks. Liang et al. [14] demonstrated the feasibility of an indirect-heating rotary kiln for pyrolyzing small-particle oil shale in an engineering experiment, highlighting its advantages such as low dust carry-over and stable operation, which provides a valuable reference for the industrial application of rotary kiln technology. Furthermore, in the context of global carbon reduction efforts, the exploration of alternative energy sources and reducing agents has become a key research direction. In a related metallurgical field, Nabilah et al. [15] investigated the reduction of saprolite nickel ore using a methane-argon gas mixture in a laboratory-scale simulated rotary kiln, exploring the feasibility of this low-carbon fuel as an alternative to traditional carbon-based reductants, thereby underscoring the potential for efficient and clean operation through parameter and energy structure optimization.

To delve into the parameter optimization mechanism, researchers have widely used numerical simulation methods such as the discrete element method (DEM) [16]. The application of DEM has proven highly effective in simulating particle systems within rotary equipment. Hu et al. [17] proposed a robust DEM framework for efficiently simulating heat generation in long-duration recurrent granular flows, providing a powerful numerical tool for

complex thermo-mechanical processes. Similarly, Wu et al. [18] combined experimental methods with computational fluid dynamics and the discrete element method (CFD-DEM) to study the drying characteristics of soil in large-scale rotary kilns, validating the applicability of DEM in coupled multiphysics field analyses. Building on this foundation, studies specific to oil shale retorting have yielded significant insights. Arntz et al. [19] used DEM to simulate the mixing and segregation inside the rotary furnace, systematically analyzing the effects of filling rate, rotational speed, and other factors on the mixing process. Wang et al. [20] combined DEM with a particle heat transfer model to study the mixing and heat transfer process of shale ash particles and oil shale particles. They used the mixing index, particle average temperature, and temperature standard deviation as evaluation indexes to analyze the influence of the filling rate, the furnace rotational speed, and the form of the baffle on the mixing and heat transfer characteristics of particles. Wang et al. [21] proposed a comprehensive heat transfer model including conduction and radiation, and used DEM to deeply analyze the effects of rotational speed and filling rate on the heating time. Xie et al. [22] employed DEM simulations to investigate rotary furnaces, revealing that the specific heat transfer coefficient of particle flows increased with rotational speed.

While DEM studies effectively reveal underlying mechanisms, they rely on complex, computationally intensive physical modeling. This makes real-time optimization of numerous coupled variables challenging. Additionally, experimental studies are limited by equipment scale and operating conditions, making it difficult to fully cover the complex working conditions under the interaction of multiple parameters.

In recent years, the rapid development of artificial intelligence (AI) technology has provided new ideas to break through the above bottlenecks. Neural-network-based prediction models can quickly establish a nonlinear mapping relationship between operating parameters and mixing and heat transfer performance by learning from a large amount of numerical simulation or experimental data. Currently, neural network algorithms are increasingly widely used in the research of rotary furnaces. By learning a large amount of simulation data and experimental data, neural networks can establish a complex relationship model between operating parameters, structural parameters, and particle mixing and heat transfer effects, and then realize the effective prediction of the performance of the rotary furnace [23, 24]. Neural networks, when integrated with intelligent algorithms such as genetic algorithms or particle swarm optimization (PSO), can achieve multi-objective parameter co-optimization [25, 26]. By establishing optimization objectives that represent mixing efficiency and heat transfer performance, these intelligent optimization algorithms can identify optimal solutions from numerous parameter combinations, thereby enabling the efficient operation of rotary furnaces.

2. Heat transfer analysis and modeling

The heat transfer between particles within the rotary furnace primarily occurs through direct contact conduction and intra-particle conduction, while the influence of interstitial fluid and radiation is considered negligible in the oxygen-free retorting environment, consistent with our previous study [27]. Therefore, a simplified particle heat conduction model, focusing on contact heat transfer, was employed in the DEM simulations.

To balance computational accuracy and efficiency, the following key assumptions were adopted: (1) particles are spherical with constant thermophysical properties; (2) the furnace wall is adiabatic; (3) the heat loss through the wall and the effect of pyrolysis volatiles on interparticle heat transfer are neglected; (4) periodic boundary conditions were applied at both ends of the reactor to simulate the axial behavior of an infinitely long rotary kiln and avoid end effects.

Based on the particle diameters (4 mm for oil shale particles and 3 mm for shale ash particles), material thermal conductivities (0.6 $W \cdot m^{-1} \cdot K^{-1}$ for oil shale and 0.9 $W \cdot m^{-1} \cdot K^{-1}$ for shale ash), and the typical effective inter-particle contact heat transfer coefficient reported in the literature (50–400 $W \cdot m^{-2} \cdot K^{-1}$) [28], the estimated Biot number ranges from approximately 0.03 to 0.44. This result indicates that the internal conductive resistance of the particles is relatively small compared to the external contact resistance between particles.

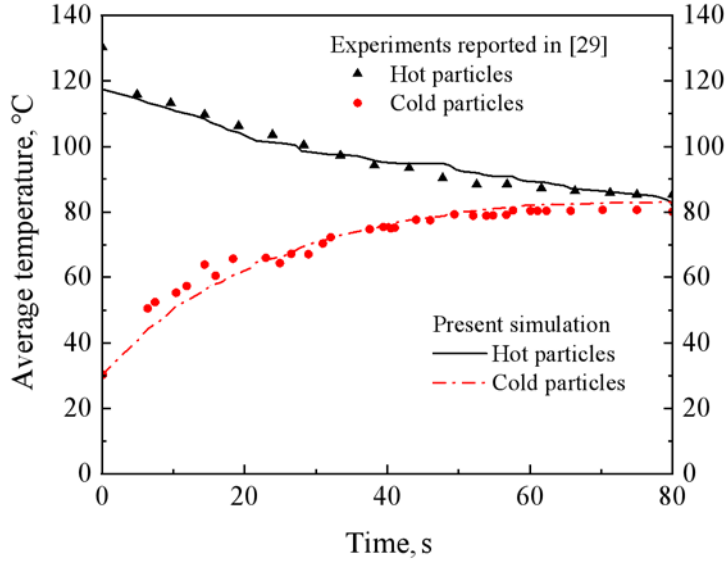

Fig. 1. Comparison between numerical simulation and experimental results for model validation.

Therefore, although the strict criterion for the lumped capacitance method (Bi << 1) is not fully satisfied at the upper end of this range, the simplified "one-temperature-per-particle" assumption employed in the present DEM model represents a reasonable and acceptable approximation for capturing system-level macroscopic heat transfer dynamics. This conclusion is further supported by experimental data from the literature [29], as shown in Figure 1. The simulated temperature evolution of the binary particle system (quartz sand and glass beads) showed good agreement with the experimental data, with the maximum relative error controlled within 9%. This confirms the model's capability to accurately capture the dynamics of particle contact heat transfer. Detailed information regarding the validation setup and material properties can be found in [27].

3. Research objects and simulation matrix

A scaled-down rotary furnace model was constructed for the DEM simulations, with key structural dimensions illustrated in Figure 2 (inner radius R_1 = 30 mm, outer radius R_2 = 32 mm, axial length L = 30 mm). The material properties for oil shale particles, shale ash particles, and the retorting wall, along with the inter-particle and particle-wall contact parameters (restitution, static, and rolling friction coefficients), were set according to the values established in our previous work (see tables 3 and 4 in [27] for details).

It should be noted that this study primarily aims to reveal fundamental mechanisms. Future work will focus on dimensional analysis and scaling laws (such as the Froude number and filling degree similarity) to facilitate the translation of these findings to industrial-scale applications.

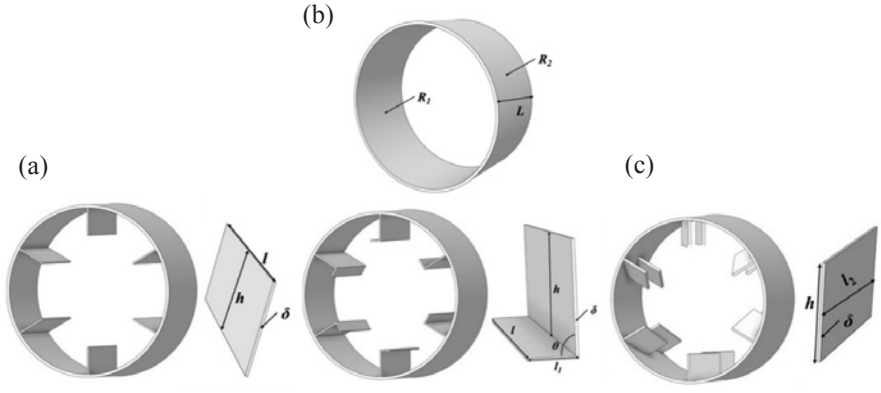

R_1 = 30 mm, R_2 = 32 mm, L = 30 mm, l = 30 mm, h = 10 mm, δ = 0.5 mm, l_1 = 4 mm, l_2 = 4 mm

Fig. 2. Structure of the baffle in the rotary furnace: straight baffle (a), right-angle baffle (b), and inclined baffle (c).

Simulations varied three key parameters – particle filling degree (20%, 30%, 50%), rotational speed (3, 4, 5 rpm), and baffle shape (straight, right-angle, inclined) – to generate the dataset for subsequent neural network training and optimization. This parametric analysis aims to systematically elucidate the influence mechanisms of these parameters on particle mixing and heat transfer characteristics. All simulated conditions maintained an initial mass ratio of 3:1 between oil shale and shale ash, with the initial temperature of shale ash (740 °C) set significantly higher than that of oil shale (110 °C) to accurately simulate the solid heat carrier process used in industrial applications.

4. Analysis of DEM simulation results

4.1. Evaluation metrics for particle mixing and heat transfer

To analyze the mixing and heat transfer between oil shale and shale ash particles, the mixing index (M), the average temperature of oil shale particles ($\overline{T}$), and the particle temperature standard deviation (S_T) were employed as evaluation metrics [26]. A higher M value indicates better mixing, while a lower S_T signifies a more uniform temperature distribution and superior heat transfer performance.

4.2. Influence of operational and structural parameters

As shown in Figure 3, a lower filling degree (20%) significantly enhanced particle mixing, achieving a higher maximum mixing index (0.217) more rapidly (112 s) compared to higher ratios (30% and 50%). This is attributed to increased particle mobility and enhanced convective mixing under reduced gravitational compaction. This observation aligns with the findings of Herz et al. [13] and Nafsun et al. [30], who also reported improved heat transfer performance at lower filling levels in rotary kilns. Although the final average temperature was similar across all cases (approximately 520 °C), the temperature distribution was markedly more uniform at the lower filling degree, as evidenced by a smaller temperature standard deviation. This indicates that reducing the filling degree improves heat transfer efficiency primarily by enhancing temperature uniformity rather than by altering the overall heating rate.

Increasing the rotational speed from 3 to 5 rpm, as illustrated in Figure 4, accelerated both the mixing rate and the heating rate of the oil shale particles. The system reached a stable mixing state more quickly at higher speeds. More importantly, the temperature standard deviation decreased significantly with increasing rotational speed, demonstrating that a higher speed effectively promotes a more homogeneous temperature field. This result is consistent with the conclusions of Xie et al. [22], who demonstrated that the specific heat transfer coefficient increases with rotational speed. At 5 rpm, the competing

effects of enhanced collision-induced mixing and incipient radial segregation led to fluctuations in the mixing index after 150 s; nevertheless, the overall heat transfer performance was superior.

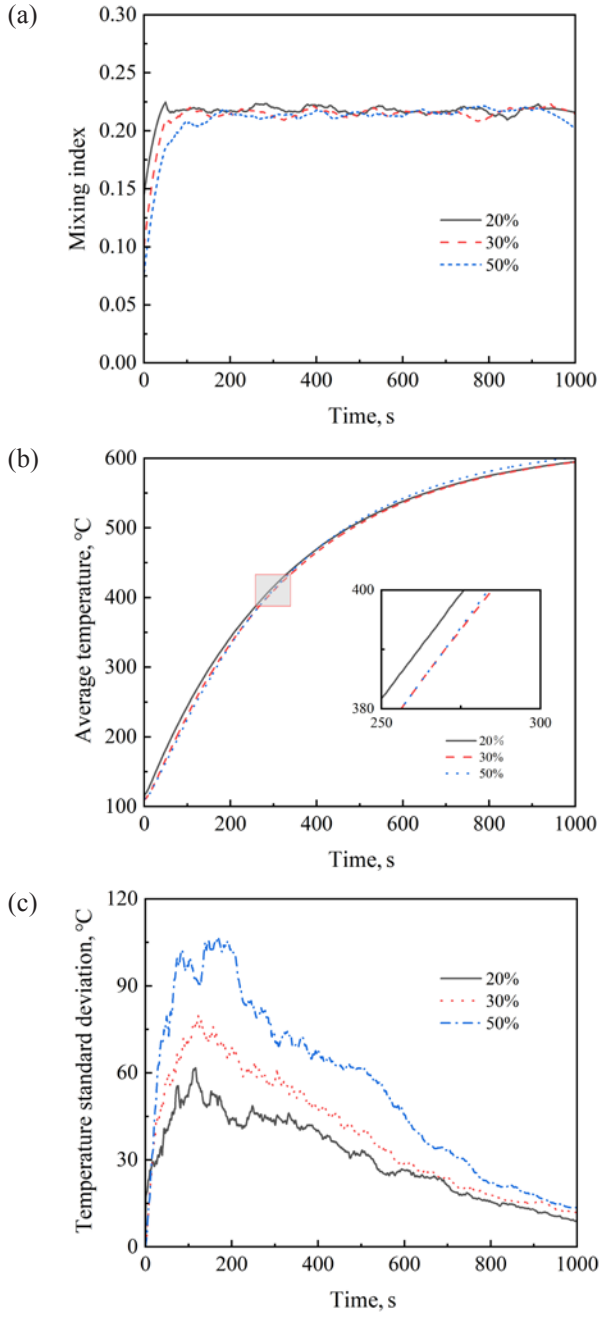

Fig. 3. Variation of evaluation indices under different filling degrees: mixing index (a), average temperature (b), and temperature standard deviation (c).

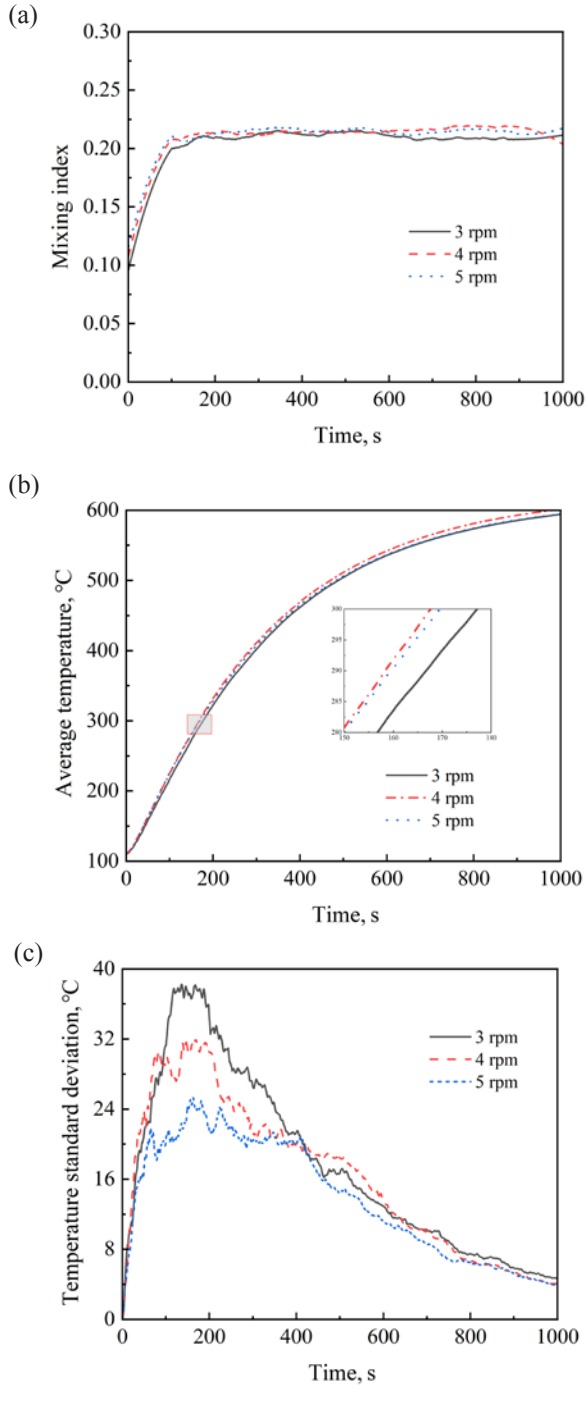

Fig. 4. Variation of evaluation indices under different rotational speeds: mixing index (a), average temperature (b), and temperature standard deviation (c).

As shown in Figure 5, the installation of baffles markedly improved mixing compared to the baffle-free structure. Among the three baffle types studied, the right-angle baffle yielded the best mixing performance ($M \approx 0.22$) and, crucially, the most uniform temperature distribution (lowest S_T). Although the straight baffle achieved a mixing index similar to that of the inclined baffle (approximately 0.21), it resulted in the largest temperature deviation. The superior performance of the right-angle baffle in achieving homogeneous mixing corroborates the experimental findings of Zhang et al. [12], who identified the right-angle baffle as optimal under specific conditions. The superior performance of the right-angle baffle stems from its ability to generate secondary vortices during particle lifting and cascading, thereby promoting radial mixing and increasing the contact frequency between hot and cold particles.

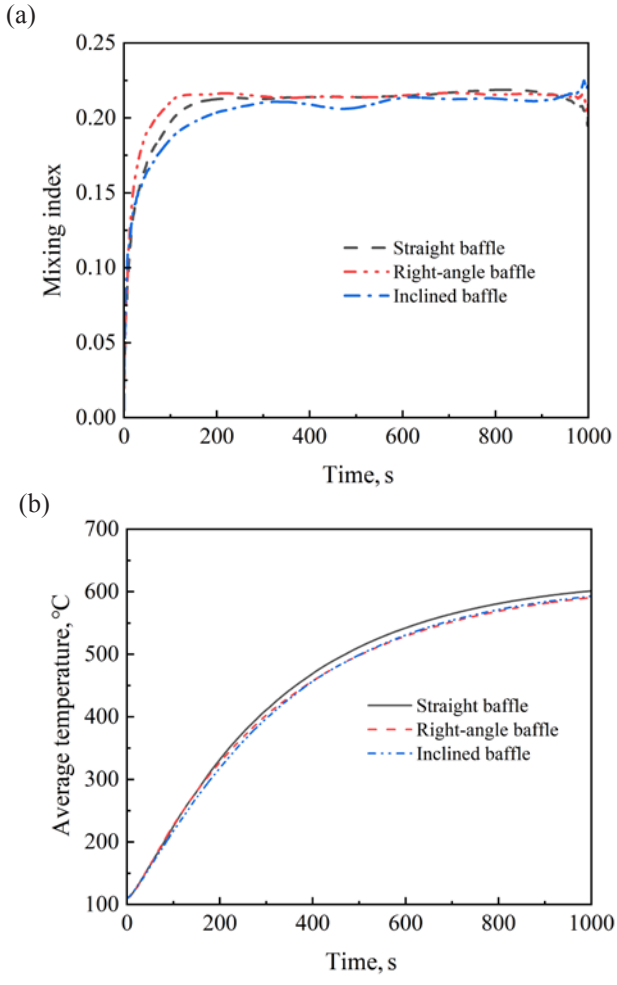

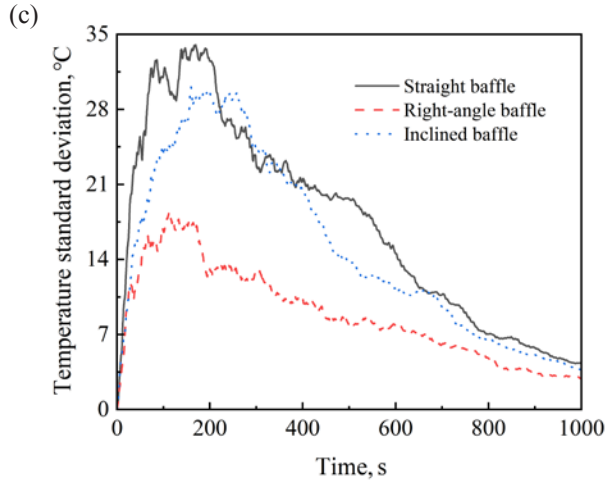

Fig. 5. Variation of evaluation indices under different baffle structures: mixing index (a), average temperature (b), and temperature standard deviation (c).

These trends are concisely summarized in Table 1, which provides a systematic comparison of how each parameter influences mixing and heat transfer performance. The synthesized results demonstrate that operational parameters (filling degree and rotational speed) predominantly affect the rate of mixing and heat transfer, as well as the uniformity of the temperature field, while structural parameters (baffle shape) play a decisive role in mixing effectiveness and thermal homogeneity. Among all configurations, the right-angle baffle combined with a lower filling degree and moderate rotational speed delivered the most favorable performance under the investigated conditions.

The results demonstrate that operational parameters (filling degree, rotational speed) primarily influence the rate of mixing and heat transfer, as well as the uniformity of the temperature field. Under the investigated conditions, the right-angle baffle was identified as the optimal design.

Table 1. Summary of the effects of key parameters on mixing and heat transfer

Parameter	Variation trend	Effect on mixing	Effect on heat transfer uniformity (S_T)
Filling degree	Decrease (50% → 20%)	Significant improvement	Significant improvement (reduces S_T)
Rotational speed	Increase (3 → 5 rpm)	Improvement (may fluctuate at high speed)	Significant improvement (reduces S_T)
Baffle type	Right-angle > inclined > straight	Right-angle is optimal	Right-angle is optimal (lowest S_T)

5. Intelligent optimization

The above analysis shows that the particle filling degree, furnace rotational speed, and baffle structure are critical parameters affecting oil shale retorting. Through genetic algorithm optimization of operating parameters, this study identifies the optimal parameter combination to achieve the best heat transfer and mixing effects for a specific baffle structure, thereby enhancing the stability and controllability of the reaction process. Optimizing operating parameters to reach the target temperature in the shortest time can significantly reduce the production cycle, improve equipment operational efficiency, and lower energy consumption and production costs.

To this end, based on DEM simulation results, this study employs backpropagation neural networks (BP-NN) and genetic algorithms to comprehensively optimize the above operating parameters and baffle structural parameters. The research is divided into two parts:

(1) BP-NN modeling: Mathematical models were established using the BP-NN neural network method to characterize the operational time of the furnace with different baffle structures in relation to filling degree, rotational speed, mixing index, and particle average temperature.

(2) Genetic algorithm optimization: With the objective of minimizing the operational time required for the furnace to reach the set target temperature (i.e., particle average temperature), operating parameters for different baffle structures – including filling degree, rotational speed, and mixing index – were optimized to facilitate better control of the reaction process.

5.1. Establishment of a training library

Using DEM simulation results under different cases, this study selected filling degree, rotational speed, mixing index, average temperature of oil shale particles, and furnace operation time data for different baffle structures. Learning samples were constructed for straight, right-angle, and inclined baffles, with sample sizes of 24901, 33173, and 41300 data points, respectively. For each baffle type, learning samples were randomly divided into test and training sets in a 1:9 ratio. Predicted operation times for test samples were obtained via neural network training and compared with their corresponding actual values.

5.2. Neural network prediction model

5.2.1. Model building

BP-NN is a multi-layer feed-forward neural network trained by the error back-propagation algorithm. It is widely used in large-scale model prediction due to its high modeling accuracy and short training time. The network consists of

an input layer, hidden layers, and an output layer, with the input signal passing through the hidden layers to the output layer.

This study employs a three-layer BP-NN, with the input layer consisting of four key parameters: filling degree, rotational speed, mixing index, and average temperature of oil shale particles. The output layer predicts the corresponding operation time. The network includes two hidden layers, each with 20 neurons. The training function is *trainbr* based on the Bayesian regularization algorithm, which reduces the overfitting risk and improves model generalization. The mean square error is used as the performance evaluation function, with a network convergence error set to 1e-6. The *tansig* activation function handles nonlinear features, while the output layer uses the *purelin* linear function to directly predict the shortest operation time.

5.2.2. Predicted results

Figure 6 shows the comparison results between predicted and actual operation times of test samples for the inclined baffle structure, along with the relative error distribution of predictions obtained via neural network training. The predicted operation times exhibit a high degree of consistency and overlap with actual values, indicating excellent prediction performance and confirming that the neural network algorithm meets the model prediction requirements of this study. Due to the large dataset, only partial comparison results are presented in Figure 6.

As shown in Figure 7, the relative error distribution of operation time predictions for the inclined baffle indicates that the relative errors of more than 90% of training samples are controlled within ±0.1%, with the maximum relative error not exceeding 0.25%. Calculations show that the average

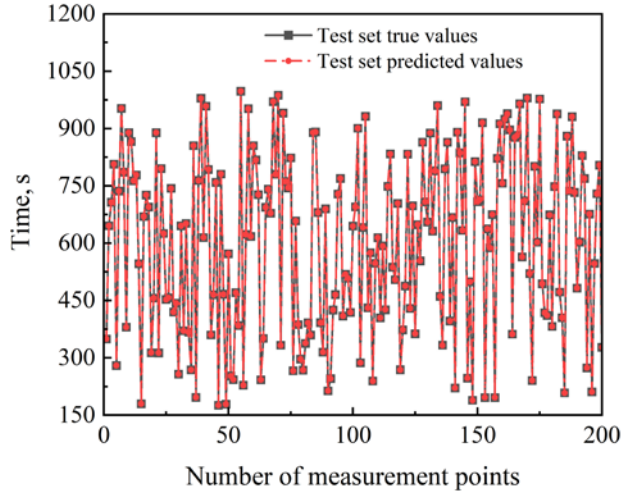

Fig. 6. Comparison between predicted and actual operation times and relative error distribution for the inclined baffle structure.

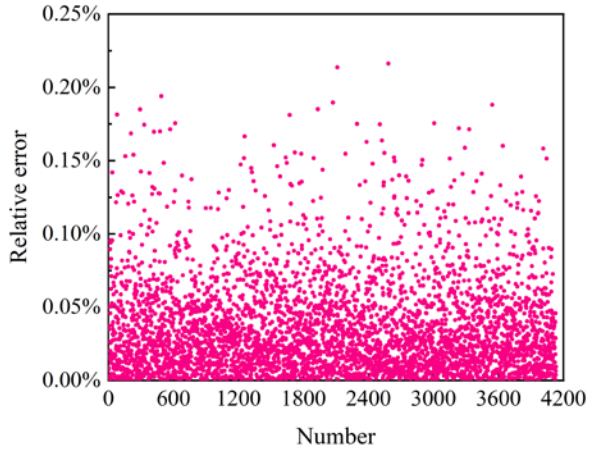

Fig. 7. Relative error of predicted operation time for inclined baffle test set.

relative errors of operation time predictions for the straight baffle, right-angle baffle, and inclined baffle are 0.03%, 0.03%, and 0.03%, respectively; all of which are less than 1%. This demonstrates that the BP-NN model accurately predicts the equipment's operation time under different operating conditions, with relative errors within the acceptable range for engineering applications.

Notably, the straight and right-angle baffle prediction samples exhibit similar operation time prediction results to the inclined baffle, and thus are not repeated here.

5.3. Genetic algorithm optimization

Genetic algorithm (GA) is a widely used global search method. The selection of an appropriate optimization algorithm is crucial for the efficiency and effectiveness of the intelligent optimization framework. Several AI-based optimization methods are available, each with distinct characteristics. For instance, PSO is renowned for its simple implementation and rapid convergence in the early stages, but it may struggle with complex multi-modal problems and is prone to premature convergence [31]. Reinforcement learning (RL) excels in sequential decision-making processes and can handle dynamic environments, yet it typically demands substantial computational resources and interaction data, which is prohibitive for computationally expensive simulations like DEM [32].

In contrast, GA was chosen for this study due to its well-established capability in handling non-linear, multi-parameter optimization problems with discontinuous and complex search spaces, which aligns well with the characteristics of our parameter-response model. Its global search ability, derived from operations such as selection, crossover, and mutation, reduces the risk of being trapped in local optima. Furthermore, the coupling of GA

with the BP-NN creates a powerful surrogate-based optimization strategy [33]. The BP-NN provides a rapid and accurate prediction of the objective function (operation time), effectively replacing the computationally intensive DEM simulations during the iterative optimization process. This GA-BP synergy offers a balanced approach between global exploration and computational efficiency for our specific problem.

In this study, the shortest running time when the equipment reaches the set temperature is taken as the optimization objective, and the filling degree, rotational speed, and mixing index of the furnace are optimized under different baffle structures. The optimization results indicate that the operation time required to reach the target temperature can be reduced by approximately 20–30% compared to the baseline conditions, which is expected to significantly lower energy consumption and production costs. In addition, increasing the heating rate can accelerate the breaking of valence bonds of organic matter, thus increasing the generation of reaction products. At the same time, rapid heating will increase the temperature gradient inside and outside the particles, which is conducive to the escape of the reaction products and shortens their residence time. This not only helps reduce secondary reactions and cracking of volatile products, ultimately improving the shale oil yield, but also contributes to enhancing the product quality of shale oil.

The parameter settings of GA are shown in Table 2.

Table 2. Optimization parameter settings in genetic algorithms

Optimization parameter	Description	Range
Objective functions	Operation time	min
Optimization variables	Particle filling degree	0.30.5
	Furnace rotational speed	3–5 rpm
	Mixing index	0.18–0.25
Constraints	Average temperature of oil shale particles	500–550 °C
Initial parameters	Generation number	100
	Population size	200
	Selection rate	Tournament
	Crossover probability	0.8
	Mutation rate	Adaptive feasible

Figure 8 illustrates the iterative evolution of fitness values during genetic algorithm optimization for minimizing operation time when the average temperature of oil shale particles reaches 520 °C under three baffle configurations: straight, right-angle, and inclined. The figure clearly reflects the convergence characteristics of the optimization process and its effect.

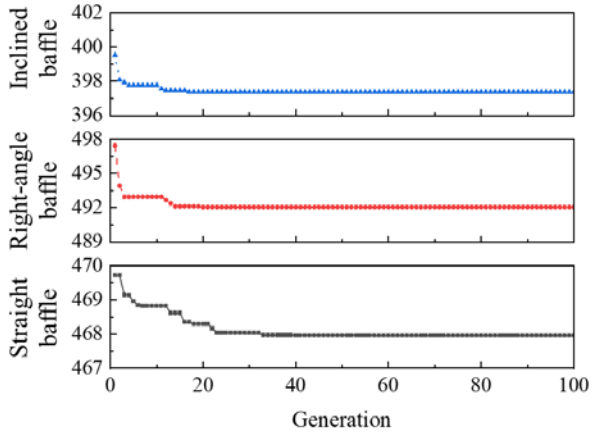

Fig. 8. Iterative optimization of fitness values for straight, right-angle, and inclined baffles at 520 °C.

From the curve trends, the algorithm rapidly improves fitness values within the first 20 generations, then enters a smooth convergence stage, and stabilizes at around 50 generations. The maximum fitness value converges to approximately 0.82.

Table 3 presents the shortest operation times and optimized parameter combinations for straight, right-angle, and inclined baffles to reach the 520 °C operating temperature. As depicted in Table 3, the inclined baffle demonstrates the highest thermal efficiency, reaching the target temperature in only 397 s, followed by the straight baffle (468 s) and the right-angle baffle (492 s). It is noteworthy that while the right-angle baffle exhibited the best mixing and temperature uniformity in the DEM analysis (Section 4.2), the inclined baffle achieved the shortest operation time in the global optimization. This highlights the distinction between optimizing for a single physical objective (e.g., mixing uniformity) and a comprehensive process objective (e.g., minimum time to reach a target temperature), and underscores the value of the integrated DEM-NN-GA framework in identifying such nuanced optimal solutions. Under optimal conditions, the mixing index of all three structural designs stabilizes at 0.18, whereas the filling degree parameters exhibit significant differences.

While traditional DEM simulations accurately analyze particle motion [17–22], they consume substantial computational resources to determine optimal conditions. In contrast, the genetic algorithm-based optimization method overcomes this limitation by establishing nonlinear mapping relationships between parameters and operation time, enabling rapid prediction of reasonable process parameter combinations and significantly improving optimization efficiency. This data-driven approach, integrating simulation with intelligent algorithms, addresses the challenge of multi-parameter coupling optimization

that is difficult to resolve through traditional numerical or experimental methods alone [15, 23]. This approach provides a new research idea and technical pathway for optimizing complex multi-parameter coupled systems.

Figure 9 illustrates the minimum operation time required for the furnace to achieve operation temperatures of 500 °C, 510 °C, 520 °C, 530 °C, 540 °C, and 550 °C for straight, right-angle, and inclined baffles. Results show that for all baffle structures, the minimum operation time increases with increasing operation temperature.

Comparing optimization results across baffle structures for the same operating temperature, the inclined baffle requires the shortest operation time, followed by the straight baffle and then the right-angle baffle. This indicates that under multi-parameter coupling, the inclined baffle exhibits the fastest

Table 3. Optimization results for straight, right-angle, and inclined baffles at 520 °C

Baffle shape	Optimization goal	Optimization variable		
	Time	Filling degree	Rotational speed, rpm	Mixing index
Straight baffle	467	0.36	5.00	0.18
Right-angle baffle	492	0.30	3.00	0.18
Inclined baffle	397	0.32	3.00	0.18

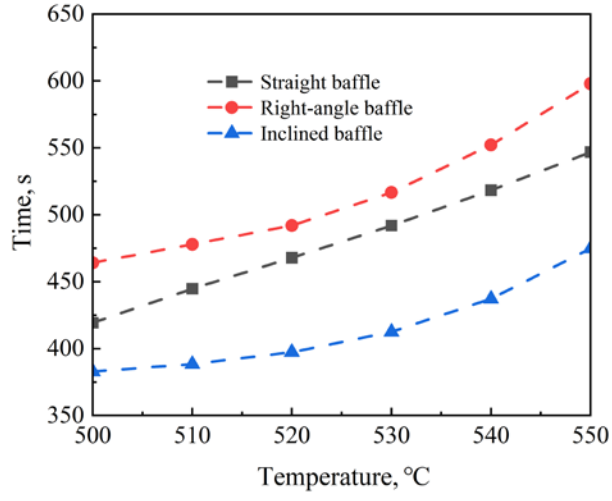

Fig. 9. Minimum operation time for straight, right-angle, and inclined baffles under different operating temperatures.

heating rate, followed by the straight baffle, with the right-angle baffle having the slowest heating rate. This finding provides a complementary perspective to the structural optimization studies exemplified by Liang et al. [14], demonstrating that the "optimal" structure can vary depending on the specific performance metric chosen for optimization.

Figure 10 shows the distribution of decision variables (filling degree, rotational speed, and mixing index) for optimizing the shortest operation time of different baffle structures under varying operating temperatures.

Figure 10(a) indicates that the filling degree for the straight baffle ranges from 0.35–0.40, decreasing with increasing operating temperature. For both the right-angle and inclined baffles, the filling degree distribution interval is 0.30–0.35. Notably, the filling degree of the right-angle baffle decreases with temperature, while that of the inclined baffle increases.

Figure 10(b) reveals that the rotational speed for the right-angle baffle ranges from 4.4–5.0 rpm. At 500 °C, the optimal condition uses 4.85 rpm, whereas other optimal conditions adopt 3.0 rpm. In contrast, the inclined baffle maintains a constant rotational speed of 3.0 rpm across all temperatures. The straight baffle's rotational speed increases with temperature, reaching 5.0 rpm at 520–550 °C. Evidently, rotational speed has a minimal impact on the minimum operation time across different baffles and temperatures.

Figure 10(c) shows that the mixing indices of the straight and right-angle baffles follow a similar trend: 0.25 at 500 °C and 0.18 at 510–550 °C. For the inclined baffle, the mixing index remains 0.18 at 500–530 °C and increases with further temperature rises. These distributions of filling degree, rotational speed, and mixing index provide a basis for equipment operation control.

(a)

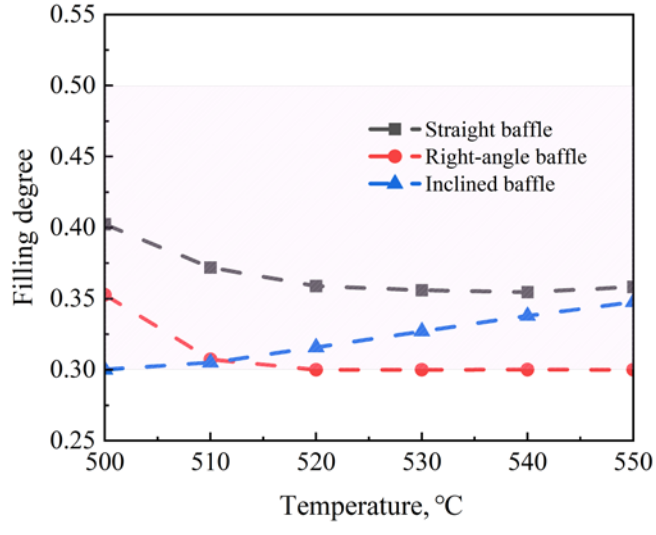

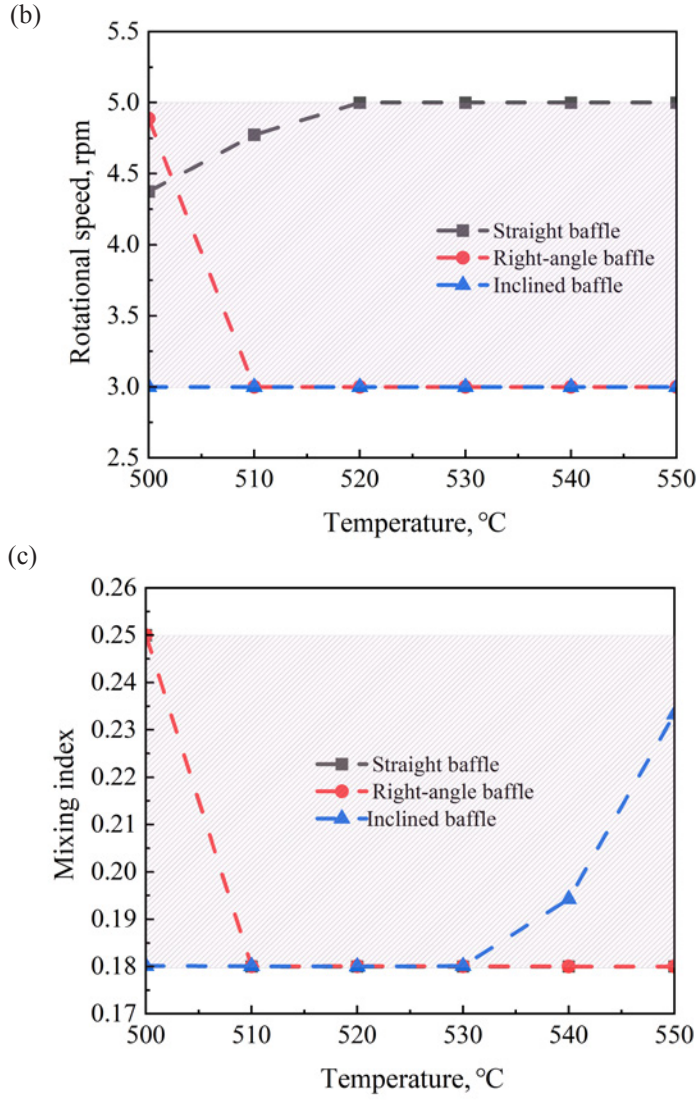

Fig. 10. Distribution of decision variables for different baffle structures under different operating temperatures: filling degree (a), rotational speed (b), and mixing index (c).

6. Conclusions

This study establishes an intelligent optimization framework for particle mixing and heat transfer in rotary retorting furnaces by integrating the discrete element method (DEM), backpropagation neural network (BP-NN), and genetic algorithm (GA). DEM simulations were first conducted to generate foundational data, based on which a BP-NN model was developed to predict

operation time. Subsequently, GA was employed for global optimization of key operational parameters to minimize the time required to reach the target temperature. The main findings are summarized as follows:

1. The established BP-NN prediction model demonstrates excellent accuracy, with a maximum relative error between predicted and actual operation times not exceeding 0.25%. This model effectively overcomes the limitations of traditional DEM simulations, such as high computational cost and long calculation time, providing an efficient tool for operational optimization.
2. The optimization framework integrating BP-NN and GA proves highly effective for multi-parameter coupling optimization in rotary retorting furnaces. By establishing a nonlinear mapping among key parameters, it enables the rapid identification of optimal settings for different baffle shapes. The results reveal a nuanced finding: while the right-angle baffle excelled in mixing and temperature uniformity in isolated analysis, the inclined baffle achieved the shortest operation time under global optimization, underscoring the importance of a system-level approach. Consequently, the optimal parameter combinations derived by GA provide clear guidance for industrial operation, promising to shorten production cycles by approximately 20–30%, reduce energy consumption, and enhance shale oil yield and quality by minimizing secondary reactions.
3. While the GA-BP framework demonstrated superior performance here, it is instructive to acknowledge its position relative to other AI paradigms. Future work could involve a comparative analysis with other meta-heuristics (e.g., particle swarm optimization) within the same surrogate-assisted framework. For scenarios requiring real-time adaptive control, exploring hybrid strategies – such as leveraging the trained network within a model-based reinforcement learning framework – presents a promising direction, despite the associated computational challenges.

Data availability statement

All data, models, and code generated or used during this study are included in the article.

Acknowledgments

This work was financially supported by the Liaoning Provincial Department of Education through a local project (No. JYTMS20231421). The publication costs of this article were partially covered by the Estonian Academy of Sciences.

References

1. Chen, B., Wu, J., Zhang, Y. Data-driven analysis and insights into sorption-induced kerogen deformation in shale. *Gas Science and Engineering*, 2025, **136**, 205579. https://doi.org/10.1016/j.jgsce.2025.205579
2. Yin, X., Cao, Z., Cao, C., Lü, N. Simulation and optimization in shale oil condensation recovery system. *Journal of Petrochemical Universities*, 2019, **32**(3), 20–27. https://doi.org/10.3969/j.issn.1006-396X.2019.03.004
3. Jia, B., Su, J. Advancements and environmental implications in oil shale exploration and processing. *Applied Sciences*, 2023, **13**(13), 7657. https://doi.org/10.3390/app13137657
4. Guo, C., Zou, T., Pan, H., Lu, H., Hu, H. Effect of transition metal salt catalysts on pyrolysis of Fushun oil shale. *Journal of Liaoning Petrochemical University*, 2021, **41**(3), 15–22. https://doi.org/10.3969/j.issn.1672-6952.2021.03.003
5. Ma, Y., Xiang, Q., Ding, K. Development of oil shale at home and abroad. *World Petroleum Industry* (China), 2024, **31**(1), 16–25. https://doi.org/10.20114/j.issn.1006-0030.20231108001
6. Li, J. *Simulation Research on Particle Heat Transfer Process in a Solid Heat Carrier Rotary Retorting for Oil Shale*. Master's thesis. Northeast Electric Power University, China, 2018.
7. Zhang, L., Wei, Q., Wang, Q. Influence of flights' shape on motion and mixing of binary particles in rotary retort. *Journal of Zhejiang University (Engineering Science)*, 2018, **52**(8), 1542–1550. https://doi.org/10.3785/j.issn.1008-973X.2018.08.014
8. Li, S., Zhang, L., Zhang, X., Yu, K., Wang, Q., Hao, W. Numerical analysis of particle mixing and movement in rotary retorting. *Proceedings of the CSEE*, 2011, **31**(2), 32–38.
9. Bisulandu, B.-J. R. M., Huchet, F. Rotary kiln process: an overview of physical mechanisms, models and applications. *Applied Thermal Engineering*, 2023, **221**, 119637. https://doi.org/10.1016/j.applthermaleng.2022.119637
10. Seidenbecher, J., Herz, F., Meitzner, C., Specht, E., Wirtz, S., Scherer, V. et al. Experimental analysis of the flight design effect on the temperature distribution in rotary kilns. *Chemical Engineering Science*, 2021, **240**, 116652.
11. He, Y., E, D., Lai, N. C., Jiang, Z. Influence of flight structures and baffle dam on particle behaviors and gas-solid heat exchange enhancement in a rotary drum. *Particuology*, 2025, **102**, 104–117. https://doi.org/10.1016/j.partic.2025.04.010
12. Zhang, L., Li, S., Yu, K., Zhang, X., Wang, Q. Cold experiments on mixing performance of oil shale particle and solid heat carrier in rotary retorting. *Chemical Industry and Engineering Progress*, 2011, **30**(3), 492–497.
13. Herz, F., Mitov, I., Specht, E., Stanev, R. Influence of operational parameters and material properties on the contact heat transfer in rotary kilns. *International Journal of Heat and Mass Transfer*, 2012, **55**(25–26), 7941–7948. https://doi.org/10.1016/j.ijheatmasstransfer.2012.08.022

14. Liang, R., Zhang, Z., Jin, Z., Yu, X., Zhang, S. Engineering application of indirect heating rotary kiln in oil shale pyrolysis treatment. *Chinese Journal of Environmental Engineering*, 2021, **15**(9), 3029–3034.
15. Nabilah, A. J., Satritama, B., Hidayat, T., Taskinen, P., Santoso, I., Kurniadani, H. et al. Reduction of saprolite nickel ore using methane-argon gas mixture with laboratory-scale simulated rotary kiln-electric furnace (RKEF) technology. *Minerals Engineering*, 2025, **234**, 109776. https://doi.org/10.1016/j.mineng.2025.109776
16. Li, J., Sun, T., Wen, L. Multi-objective evaluation of optimization of direct evaporative cooling air supply mode in rotary kiln process section. *Refrigeration and Air Conditioning*, 2025, **39**(1), 56–65.
17. Hu, J., Zhang, L., Wang, B., Kisuka, F., He, Y., Wang, Z. et al. A robust DEM framework for efficient simulation of heat generation in long-duration recurrent granular flows. *Powder Technology*, 2025, **465**, 121308. https://doi.org/10.1016/j.powtec.2025.121308
18. Wu, H., Li, W., Wang, J., Zhan, M., Gu, H., Xu, P. et al. Drying characteristics of soil in large-scale rotary kilns: an experimental and CFD-DEM study. *Drying Technology*, 2025, **43**(3), 527–540. https://doi.org/10.1080/07373937.2024.2436505
19. Arntz, M. M. H. D., den Otter, W. K., Briels, W. J., Bussmann, P. J. T., Beeftink, H. H., Boom, R. M. Granular mixing and segregation in a horizontal rotating drum: a simulation study on the impact of rotational speed and fill level. *AIChE Journal*, 2010, **54**(12), 3133–3146. https://doi.org/10.1002/aic.11622
20. Wang, Q., Li, J., Wang, Z., Zhang, L. Numerical simulation on characteristics of heat transfer between particles in rotary retorting. *CIESC Journal*, 2017, **68**(11), 4137–4146. https://doi.org/10.11949/j.issn.0438-1157.20170147
21. Wang, Q., Liu, B. W., Wang, Z. C. Investigation of heat transfer mechanisms among particles in horizontal rotary retorts. *Powder Technology*, 2020, **367**, 82–96. https://doi.org/10.1016/j.powtec.2020.03.042
22. Xie, Q., Chen, Z. B., Hou, Q. F., Yu, A. B., Yang, R. DEM investigation of heat transfer in a drum mixer with lifters. *Powder Technology*, 2017, **314**, 175–181. https://doi.org/10.1016/j.powtec.2016.09.022
23. Wang, M., Chen, E., Liu, P., Guo, W. Multivariable nonlinear predictive control of a clinker sintering system at different working states by combining artificial neural network and autoregressive exogenous. *Advances in Mechanical Engineering*, 2020, **12**(1), 1687814019896509. https://doi.org/10.1177/1687814019896509
24. Li, T., Zhang, Z., Chen, H. Predicting the combustion state of rotary kilns using a convolutional recurrent neural network. *Journal of Process Control*, 2019, **84**, 207–214. https://doi.org/10.1016/j.jprocont.2019.10.009
25. Ko, M. S., Chang, T. B., Lee, C. Y., Huang, J. W., Lim, C. F. Optimization of cyclone-type rotary kiln reactor for carbonation of BOF slag. *Sustainability*, 2021, **13**(20), 11556. https://doi.org/10.3390/su132011556

26. Zhang, R. F. *Research on State Recognition and Intelligent Optimization Method of Cement Clinker Calcination Process*. PhD thesis. University of Jinan, China, 2023.
27. Wang, C., Sun, Y., Wang, N., Sun, J., Yue, Y. Study on the influence of baffles on heat transfer characteristics of particles in an oil shale rotary kiln. *Applied Thermal Engineering*, 2025, **268**, 125924. https://doi.org/10.1016/j.applthermaleng.2025.125924
28. Zhou, Z. Y., Yu, A. B., Zulli, P. Particle scale study of heat transfer in packed and bubbling fluidized beds. *AIChE Journal*, 2009, **55**(4), 868–884. https://doi.org/10.1002/aic.11823
29. Chaudhuri, B., Muzzio, F. J., Tomassone, M. S. Modeling of heat transfer in granular flow in rotating vessels. *Chemical Engineering Science*, 2006, **61**(19), 6348–6360. https://doi.org/10.1016/j.ces.2006.05.034
30. Nafsun, A. I., Herz, F., Liu, X. Influence of material thermal properties and dispersity on thermal bed mixing in rotary drums. *Powder Technology*, 2018, **331**, 121–128. https://doi.org/10.1016/j.powtec.2018.01.072
31. Kant, R., Maurya, S. P., Singh, K. H. Qualitative and quantitative reservoir characterization using seismic inversion based on particle swarm optimization and genetic algorithm: a comparative case study. *Scientific Reports*, 2024, **14**(1), 22581. https://doi.org/10.21203/rs.3.rs-3141822/v1
32. Michailidis, P., Michailidis, I., Kosmatopoulos, E. Reinforcement learning for optimizing renewable energy utilization in buildings: a review on applications and innovations. *Energies*, 2025, **18**(7), 1724. https://doi.org/10.3390/en18071724
33. Jin, L., Duan, J., Fan, T., Jiao, P., Dong, T., Wu, Q. Using GA-BP coupling algorithm to predict the high-performance concrete mechanical property. *KSCE Journal of Civil Engineering*, 2023, **27**(2), 684–697. https://doi.org/10.1007/s12205-022-0912-9